

1 **TITLE**

2 Low coverage whole genome sequencing enables accurate assessment of common variants  
3 and calculation of genome-wide polygenic scores

4

5 **AUTHORS AND AFFILIATIONS**

6 Julian R. Homburger,<sup>1</sup> Cynthia L. Neben,<sup>1</sup> Gilad Mishne,<sup>1</sup> Alicia Y. Zhou,<sup>1</sup> Sekar Kathiresan,<sup>2-4</sup>  
7 Amit V. Khera<sup>2-4</sup> \*

8

9 <sup>1</sup>Color Genomics, 831 Mitten Road, Suite 100, Burlingame, CA, 94010 USA

10 <sup>2</sup>Center for Genomic Medicine and Cardiology Division, Department of Medicine, Massachusetts  
11 General Hospital, Boston, MA, 02114 USA

12 <sup>3</sup>Cardiovascular Disease Initiative of the Broad Institute of MIT and Harvard, Cambridge, MA,  
13 02142 USA

14 <sup>4</sup>Harvard Medical School, Boston, MA, 02115 USA

15

16 **CORRESPONDING AUTHOR**

17 \*Amit V. Khera, MD, MSc

18 Center for Genomic Medicine

19 Massachusetts General Hospital

20 Simches Research Building | CPZN 6.256

21 Boston, MA 02114 USA

22 Tel: 617.726.7876

23 Email: [avkhera@mgh.harvard.edu](mailto:avkhera@mgh.harvard.edu)

24

25 **ABSTRACT**

26 **Background:** The inherited susceptibility of common, complex diseases may be caused by  
27 rare, 'monogenic' pathogenic variants or by the cumulative effect of numerous common,  
28 'polygenic' variants. As such, comprehensive genome interpretation could involve two distinct  
29 genetic testing technologies -- high coverage next generation sequencing for known genes to  
30 detect pathogenic variants and a genome-wide genotyping array followed by imputation to  
31 calculate genome-wide polygenic scores (GPSs). Here we assessed the feasibility and  
32 accuracy of using low coverage whole genome sequencing (lcWGS) as an alternative to  
33 genotyping arrays to calculate GPSs.

34

35 **Methods:** First, we performed downsampling and imputation of WGS data from ten individuals  
36 to assess concordance with known genotypes. Second, we assessed the correlation between  
37 GPSs for three common diseases -- coronary artery disease (CAD), breast cancer (BC), and  
38 atrial fibrillation (AF) -- calculated using lcWGS and genotyping array in 184 samples. Third, we  
39 assessed concordance of lcWGS-based genotype calls and GPS calculation in 120 individuals  
40 with known genotypes, selected to reflect diverse ancestral backgrounds. Fourth, we assessed  
41 the relationship between GPSs calculated using lcWGS and disease phenotypes in 11,502  
42 European individuals seeking genetic testing.

43

44 **Results:** We found imputation accuracy  $r^2$  values of greater than 0.90 for all ten samples --  
45 including those of African and Ashkenazi Jewish ancestry -- with lcWGS data at 0.5X. GPSs  
46 calculated using both lcWGS and genotyping array followed by imputation in 184 individuals  
47 were highly correlated for each of the three common diseases ( $r^2 = 0.93 - 0.97$ ) with similar  
48 score distributions. Using lcWGS data from 120 individuals of diverse ancestral backgrounds,  
49 including South Asian, East Asian, and Hispanic individuals, we found similar results with  
50 respect to imputation accuracy and GPS correlations. Finally, we calculated GPSs for CAD, BC,

51 and AF using lcWGS in 11,502 European individuals, confirming odds ratios per standard  
52 deviation increment in GPSs ranging 1.28 to 1.59, consistent with previous studies.

53

54 **Conclusions:** Here we show that lcWGS is an alternative approach to genotyping arrays for  
55 common genetic variant assessment and GPS calculation. lcWGS provides comparable  
56 imputation accuracy while also overcoming the ascertainment bias inherent to variant selection  
57 in genotyping array design.

58

59 **KEYWORDS**

60 Genome-wide polygenic score; low coverage whole genome sequencing; coronary artery  
61 disease; breast cancer; atrial fibrillation

## 62 BACKGROUND

63 Cardiovascular disease and cancer are common, complex diseases that remain leading causes  
64 of global mortality [1]. Long recognized to be heritable, recent advances in human genetics have  
65 led to consideration of DNA-based risk stratification to guide prevention or screening strategies.  
66 In some cases, such conditions can be caused by rare, 'monogenic' pathogenic variants that  
67 lead to a several-fold increased risk -- important examples are pathogenic variants in *LDLR* that  
68 cause familial hypercholesterolemia and pathogenic variants in *BRCA1* and *BRCA2* that  
69 underlie hereditary breast and ovarian cancer syndrome. However, the majority of individuals  
70 afflicted with these diseases do not harbor any such pathogenic variants. Rather, the inherited  
71 susceptibility of many complex traits and diseases is often 'polygenic,' driven by the cumulative  
72 effect of numerous common variants scattered across the genome [2].

73

74 Genome-wide polygenic scores (GPSs) provide a way to integrate information from numerous  
75 sites of common variation into a single metric of inherited susceptibility and are now able to  
76 identify individuals with a several-fold increased risk of common, complex diseases, including  
77 coronary artery disease (CAD), breast cancer (BC), and atrial fibrillation (AF) [3]. For example,  
78 for CAD, we noted that 8% of the population inherits more than triple the normal risk on the  
79 basis of polygenic variation, a prevalence more than 20-fold higher than monogenic familial  
80 hypercholesterolemia variants in *LDLR* that confer similar risk [3].

81

82 Comprehensive genome interpretation for common, complex disease therefore could involve  
83 both high-fidelity sequencing of important driver genes to identify potential monogenic risk  
84 pathogenic variants and a survey of all common variants across the genome to enable GPS  
85 calculation. High coverage whole genome sequencing (hcWGS; for example, 30X coverage) will  
86 likely emerge as a single genetic testing strategy, but current prices remain a barrier to large-  
87 scale adoption. Instead, the traditional approach has mandated use of two distinct genetic

88 testing technologies -- high coverage next generation sequencing (NGS) of important genes to  
89 detect pathogenic variants and a genome-wide genotyping array followed by imputation to  
90 calculate GPSs.

91  
92 Low coverage whole genome sequencing (lcWGS; for example, 0.5X coverage) followed by  
93 imputation is a potential alternative approach to genotyping arrays for assessing the common  
94 genetic variants needed for GPS calculations. Several recent studies have demonstrated the  
95 efficiency and accuracy of lcWGS for other applications of statistical genetics, including local  
96 ancestry deconvolution, complex trait association studies, and detection of rare genetic variants  
97 [4–7].

98  
99 We developed a pipeline for common genetic variant imputation using lcWGS data on samples  
100 from the 1000 Genomes Project (1KGP) and Genome in a Bottle (GIAB) Consortium and herein  
101 demonstrate imputation accuracy for lcWGS similar to genotyping arrays. Using three recently  
102 published GPSs for CAD [3], BC [8], and AF [3], we show high technical concordance in GPSs  
103 calculated from lcWGS and genotyping arrays. Finally, using our pipeline in a large European  
104 population seeking genetic testing, we observe similar GPS risk stratification performance as  
105 previously published array-based results [3,8].

106

## 107 **METHODS**

### 108 **Study design**

109 The study design is summarized in Figure 1 and described in detail below. The pipeline  
110 validation data set (n = 10) was used to assess imputation accuracy for common genetic  
111 variants (Figure 1A). The technical concordance cohort (n = 184) was used to assess the  
112 correlation between three previously published GPSs for CAD [3], BC [8], and AF [3] from  
113 lcWGS and genotyping arrays (Figure 1B). The diverse ancestry data set (n = 120) was used to

114 assess imputation accuracy for common genetic variants and performance of GPS<sub>CAD</sub>, GPS<sub>BC</sub>,  
115 and GPS<sub>AF</sub> (Figure 1B). The clinical cohort (n = 11,502) was used to assess performance of  
116 GPS<sub>CAD</sub>, GPS<sub>BC</sub>, and GPS<sub>AF</sub> in a large European population seeking genetic testing (Figure 1B).

117

### 118 **Data set and cohort selection**

119 The pipeline validation data set included seven globally representative samples from 1KGP  
120 populations (HG02155, NA12878, HG00663, HG01485, NA21144, NA20510, and NA19420;  
121 see Supplementary Table 1, Additional File 1) and a trio of Ashkenazi samples (NA24385,  
122 NA24143, and NA24149) from the GIAB Consortium (Figure 1A).

123

124 The technical concordance cohort included DNA samples from 184 individuals whose  
125 healthcare provider had ordered a Color multi-gene panel test (Figure 1B). All individuals 1) had  
126 85% or greater European genetic ancestry calculated using fastNGSadmix [9] using 1KGP as  
127 the reference panel, 2) self-identified as 'Caucasian', and 3) did not have pathogenic or likely  
128 pathogenic variants in the multi-gene NGS panel test, as previously described [10] (see  
129 Supplementary Methods, Additional File 2). Demographics are provided in Supplementary Table  
130 2, Additional File 1. All phenotypic information was self-reported by the individual through an  
131 online, interactive health history tool. Of the 184 individuals, 61 individuals reported having a  
132 personal history of CAD (defined here as a myocardial infarction or coronary artery bypass  
133 surgery), 62 individuals reported no personal history of CAD, and 61 individuals reported no  
134 personal history of CAD but were suspected to have a high GPS<sub>CAD</sub> based on preliminary  
135 analysis. This preliminary analysis included imputation from multi-gene panel and off-target  
136 sequencing data, which has been shown to have similar association statistics and effect sizes  
137 compared to genotyping arrays [4]. These individuals were included in the technical  
138 concordance cohort to artificially create a relatively uniform distribution of GPS<sub>CAD</sub> in the data  
139 set. Correlation coefficients between GPS<sub>CAD</sub> from lcWGS and genotyping array were calculated

140 after removing the 61 individuals who were suspected to have a high GPS<sub>CAD</sub> based on multi-  
141 gene panel and off-target sequencing data to avoid artificial inflation of the correlation  
142 coefficient. Two individuals who reported no personal history of CAD but were suspected to  
143 have a high GPS<sub>CAD</sub> failed genotyping (quality control call rate of < 97%) and lcWGS (overall  
144 coverage of < 0.5X), leaving a total of 182 individuals for analyses.

145  
146 The diverse ancestry data set included a total of 120 samples from the following populations  
147 from 1KGP: Han Chinese in Beijing, China (CHB); Yoruba in Ibadan, Nigeria (YRI); Gujarati  
148 Indian from Houston, Texas (GIH); Americans of African Ancestry in Southwest USA (ASW);  
149 Mexican Ancestry from Los Angeles, USA (MXL); and Puerto Ricans from Puerto Rico (PUR)  
150 (see Supplementary Table 3, Additional File 1; Figure 1B). Four samples, including NA18917  
151 and NA19147 from the YRI population and NA19729 and NA19785 from the MXL population,  
152 were below the target 0.5X coverage and removed from analyses.

153  
154 The clinical cohort included DNA samples from 11,502 individuals whose healthcare provider  
155 had ordered a Color multi-gene panel test (Figure 1B). All individuals 1) had 90% or greater  
156 European genetic ancestry calculated using fastNGSadmix [9] using 1KPG as the reference  
157 panel, 2) self-identified as 'Caucasian', 3) provided history of whether they had a clinical  
158 diagnosis of CAD, BC, or AF, and 4) did not have pathogenic or likely pathogenic variants  
159 detected in the multi-gene NGS panel test, as previously described [10] (see Supplementary  
160 Methods, Additional File 2). Demographics are provided in Supplementary Table 2, Additional  
161 File 1. All phenotypic information was self-reported by the individual through an online,  
162 interactive health history tool.

163

164 **Whole genome sequencing**

165 DNA was extracted from blood or saliva samples and purified using the Perkin Elmer Chemagic  
166 DNA Extraction Kit (Perkin Elmer, Waltham, MA) automated on the Hamilton STAR (Hamilton,  
167 Reno, NV) and the Chemagic Liquid Handler (Perkin Elmer, Waltham, MA). The quality and  
168 quantity of the extracted DNA were assessed by UV spectroscopy (BioTek, Winooski, VT). High  
169 molecular weight genomic DNA was enzymatically fragmented and prepared using the Kapa  
170 HyperPlus Library Preparation Kit (Roche Sequencing, Pleasanton, CA) automated on the  
171 Hamilton Star liquid handler and uniquely tagged with 10 bp dual-unique barcodes (IDT,  
172 Coralville, IA). Libraries were pooled together and loaded onto the NovaSeq 6000 (Illumina, San  
173 Diego, CA) for 2 x 150 bp sequencing.

174  
175 For the pipeline validation data set, all samples underwent WGS with mean coverage of 13.22X  
176 (range 7.82X to 17.30X); downsampling was then performed using SAMtools to simulate  
177 lcWGS. For the technical concordance cohort, all samples underwent lcWGS with mean  
178 coverage of 1.24X (range 0.54X to 1.76X). Imputed genotypes were compared with published,  
179 high-confidence known genotypes from 1KGP and the GIAB Consortium. For the diverse  
180 ancestry data set, all samples underwent lcWGS with mean coverage of 0.89X (range 0.68X to  
181 1.24X). For the clinical cohort, all samples underwent lcWGS with mean coverage of 0.95X  
182 (range 0.51X to 2.57X).

183

#### 184 **Downsampling**

185 For the pipeline validation data set, aligned reads were downsampled using SAMtools [11] to  
186 2.0X, 1.0X, 0.75X, 0.5X, 0.4X, 0.25X, and 0.1X coverage. For the technical concordance cohort,  
187 aligned reads were downsampled to 1.0X, 0.75X, 0.5X, 0.4X, 0.25X, and 0.1X coverage. In a  
188 few cases in the technical concordance cohort, the primary samples had fewer reads than the  
189 target downsample. In those situations, all of the reads were retained. For example, if the  
190 primary sample only had 0.8X coverage, when downsampled to 1.0X, all reads were retained.



191 Downsampling was repeated using two independent seeds in SAMtools. Once the  
192 downsampled data was generated, the imputation was repeated to generate imputed genotypes  
193 using only the downsampled reads.

194

#### 195 **Imputation site selection**

196 All data sets and cohorts were imputed to a set of autosomal SNP and insertion-deletion (indel)  
197 sites from 1KGP with greater than 1% allele frequency in any of the five 1KGP super  
198 populations (African, American, East Asian, European, and South Asian), for a total of  
199 21,770,397 sites. This is hereafter referred to as the 'imputation SNP loci.' Multi-allelic SNPs  
200 and indels were represented as two biallelic markers for imputation.

201

#### 202 **Genotype likelihood calculations and imputation**

203 Genotype likelihood calculations and imputation were performed independently for each  
204 sample. Sequence reads were aligned with the human genome reference GRCh37.p12 using  
205 the Burrows-Wheeler Aligner (BWA) [12], and duplicate and low quality reads were removed.  
206 Genotype likelihoods were then calculated at each of the biallelic SNP loci in the imputation  
207 SNP loci that were covered by one or more sequencing reads called using the mpileup  
208 command implemented in bcftools version 1.8 [13]. Indels or multi-allelic sites were not included  
209 in this first genotype likelihood calculation. Reads with a minimum mapping alignment quality of  
210 10 or greater and bases with a minimum base quality of 10 or greater were included. Genotype  
211 likelihoods at each observed site were then calculated using the bcftools call command with  
212 allele information corresponding to the imputation SNP loci. This procedure discarded calls with  
213 indels or calls where the observed base did not match either the reference or expected alternate  
214 allele for the SNP locus.

215

216 Imputation was performed using the genotype likelihood imputation option implemented in  
217 BEAGLE 4.1 [14]. This imputation used default parameters except with a model scale  
218 parameter of 2 and the number of phasing iterations to 0. A custom reference panel was  
219 constructed for each sample being imputed by selecting the 250 most similar samples to that  
220 sample from 1KGP Phase 3 release using Identity-by-State (IBS) comparison. A reference  
221 panel size of 250 was selected to best balance imputation run time and accuracy (see  
222 Supplementary Figure 1, Additional File 2). To ensure that IBS values were comparable across  
223 samples, a set of regions consistently sequenced at high depth (> 20X) across all samples was  
224 utilized. When imputation was performed on samples included in 1KGP Phase 3 release, that  
225 sample and any related samples were excluded from the custom reference panel.

226

227 To generate genotypes at all of the remaining untyped sites, a second round of imputation was  
228 performed using BEAGLE 5.0 [15]. This imputation used default settings and included the full  
229 1KGP as the imputation reference panel. To note, when performing analysis using 1KGP  
230 samples, any related individuals were removed. Each sample then had imputed genotype calls  
231 at each of the imputation SNP loci. Indels and multiallelic sites were included in this second  
232 genotype likelihood calculation.

233

### 234 **Genotyping array**

235 DNA was extracted from blood or saliva samples and purified using the Perkin Elmer Chemagic  
236 DNA Extraction Kit (Perkin Elmer, Waltham, MA) automated on the Hamilton STAR (Hamilton,  
237 Reno, NV) and the Chemagic Liquid Handler (Perkin Elmer, Waltham, MA). The quality and  
238 quantity of the extracted DNA were assessed by UV spectroscopy (BioTek, Winooski, VT).

239

240 DNA was genotyped on the Axiom UK Biobank Array by Affymetrix (Santa Clara, CA).

241 Genotypes were filtered according to the manufacturer's recommendations, removing loci with

242 greater than 5% global missingness and those that significantly deviated from Hardy-Weinberg  
243 equilibrium. In addition, all A/T and G/C SNPs were removed due to potential strand  
244 inconsistencies. Each of the remaining SNPs were aligned with the hg19 reference sequence to  
245 correctly code the reference alleles as allele 1, matching the sequencing data.

246

247 To generate genotypes at all of the remaining untyped sites, imputation was performed using  
248 BEAGLE 5.0 [15]. This imputation used default settings and included the full 1KGP as the  
249 imputation reference panel. To note, when performing analysis using 1KGP samples, any  
250 related individuals were removed. Each sample then had imputed genotype calls at each of the  
251 imputation SNP loci.

252

### 253 **Imputation accuracy and quality assessment**

254 Imputation accuracy for 1KGP and GIAB samples was calculated by comparing imputation  
255 results with previously released genotypes, excluding regions marked as low confidence by  
256 GIAB.

257

258 Imputation accuracy on the genotyped samples was assessed on 470,363 sites that were  
259 included on the genotyping array at different allele frequency buckets: 257,362 sites with greater  
260 than 5% allele frequency, 119,978 sites between 1-5% allele frequency, and 93,022 sites with  
261 less than 1% allele frequency. Imputation quality was assessed through site-specific dosage  $r^2$   
262 comparing with genotype values from the genotyping array.

263

### 264 **GPS selection**

265 The GPSs for CAD [3], BC [8], and AF [3] were previously published and selected based on  
266 their demonstrated ability to accurately predict and stratify disease risk as well as identify  
267 individuals at risk comparable to monogenic disease. GPS<sub>CAD</sub> contained 6,630,150

268 polymorphisms, GPS<sub>BC</sub> contained 3,820 polymorphisms, and GPS<sub>AF</sub> contained 6,730,541  
269 polymorphisms. All loci included in these scores were included in the imputation SNP loci.

270

## 271 **GPS normalization**

272 In the clinical cohort, raw GPSs were normalized by taking the standardized residual of the  
273 predicted score after correction for the first 10 principal components (PC) of ancestry [16]. PCs  
274 were calculated by projecting lcWGS samples into 10 dimensional PC analysis (PCA) space  
275 using the LASER program [17]. A combination of samples from 1KGP and the Human Origins  
276 [18] project were used as a reference for the projection.

277

## 278 **RESULTS**

### 279 **Development and validation of imputation pipeline for lcWGS**

280 Previous studies have evaluated the potential use of lcWGS in local ancestry deconvolution,  
281 complex trait association studies, and detection of rare genetic variants [4–6]. To assess the  
282 feasibility and accuracy of this approach for GPSs, we first developed an imputation pipeline  
283 that reads raw fastq sequence data and generates a vcf with imputed site information at 21.7  
284 million sites (imputation SNP loci) (Figure 1A, B). Briefly, reads are aligned to the reference  
285 genome and filtered for duplicates and low quality. Using this BAM file, we then calculate  
286 genotype likelihoods and impute expected genotypes using 1KGP as the imputation reference  
287 panel.

288

289 To validate this imputation pipeline, we performed hcWGS and downsampling on seven  
290 samples from different 1KGP populations and a trio of Ashkenazi Jewish GIAB samples  
291 (pipeline validation data set) to varying depths of coverage from 2.0X to 0.1X (See  
292 Supplementary Table 1, Additional File 2). We used the published genotype calls for each of  
293 these samples as truth data and found that imputation accuracy was above 0.90  $r^2$  for all

294 samples at 0.5X and higher (Figure 2). As expected, this was correlated with sequencing depth,  
295 with diminishing gains observed at coverages above 1.0X. While imputation accuracy was  
296 similar across diverse populations, it was slightly reduced in the Colombian sample (HG01485),  
297 likely due to complex local ancestry related to admixture, and in the Yoruban sample  
298 (NA19240), likely due to the shorter blocks of linkage disequilibrium and higher genetic diversity  
299 in Africa [19]. Taken together, these data suggest that at sequencing depth at or above 0.5X,  
300 our pipeline has similar imputation accuracy to genotyping array-based imputation across  
301 individuals from multiple populations. As such, we set 0.5X as a quality control for success and  
302 removed samples with coverage below this threshold in subsequent analyses.

303

#### 304 **Technical concordance between GPSs calculated from lcWGS and genotyping array**

305 To assess the technical concordance of using lcWGS to calculate GPSs, we performed low  
306 coverage sequencing and used genotyping arrays on DNA from 184 individuals (technical  
307 concordance cohort) (Figure 1B). This concordance assessment was restricted to individuals of  
308 European ancestry to most closely align with the populations used for GPS training and  
309 validation.

310

311 We first compared the lcWGS genotype dosages with a subset of variants directly genotyped ( $n$   
312 = 470,362) on the genotyping array to assess imputation performance. Assuming the typed loci  
313 called on the genotyping array as ‘true’, we observed an average imputation  $r^2 > 0.90$  at 0.5X  
314 depth for variants with global minor allele frequency (MAF) greater than 5% (see Supplementary  
315 Figure 2, Additional File 3). As expected, imputation accuracy was highest for variants with  
316 higher MAF. For lower frequency variants, we saw a reduction in imputation accuracy, as  
317 expected, with  $r^2 > 0.85$  for variants at 1% to 5% MAF and  $r^2 > 0.80$  for variants less than 1%  
318 global MAF. Taken together, this demonstrates that lcWGS has high accuracy in this test  
319 setting.

320

321 We then calculated previously published GPSs for CAD [3], BC [8], and AF [3] on each sample  
322 using genotyping array data or lcWGS data. We found that  $GPS_{CAD}$ ,  $GPS_{BC}$ , and  $GPS_{AF}$  were  
323 highly correlated (Figure 3A-C), with the score mean (Student t-test  $p = 0.17$ ) and variance (F  
324 test  $p = 0.91$ ) equivalent between lcWGS and the genotyping array. The correlations of  $GPS_{CAD}$   
325 and  $GPS_{AF}$  ( $r^2 = 0.98$  and  $r^2 = 0.97$ , respectively) were slightly higher than that of  $GPS_{BC}$  ( $r^2 =$   
326  $0.93$ ), which could be due to 1) the smaller number of loci in  $GPS_{BC}$  (6.6 million compared to  
327 3820 SNPs), 2) differences in allele frequencies between SNPs with high weights, and/or 3) the  
328 fact that  $GPS_{BC}$  was trained and validated on a different genotyping array, the OncoArray, than  
329 the Axiom UK Biobank Array used in this study [8].

330

331 The technical concordance cohort ranged in coverage from 0.54X to 1.76X with a mean  
332 coverage of 1.24X, and we have shown that depth can impact imputation performance -- depth  
333 increases above 0.5X have a smaller but measurable effect on imputation performance (Figure  
334 2; see Supplementary Figure 2, Additional File 3). To determine the low coverage sequencing  
335 depth required for GPS accuracy, we used SAMtools to downsample the lcWGS data in this  
336 cohort to 1.0X, 0.75X, 0.5X, 0.4X, 0.25X, and 0.1X. We found that  $GPS_{CAD}$ ,  $GPS_{BC}$ , and  $GPS_{AF}$   
337 are robust to lcWGS sequencing depth 0.5X and that coverages do not systematically bias GPS  
338 calculations in a specific direction (see Supplementary Figure 3 and Supplementary Figure 4,  
339 Additional File 3), indicating that samples above 0.5X with small changes in coverage variation  
340 can be combined for downstream analysis. In addition, the correlation increases logarithmically  
341 as coverage increases (see Supplementary Figure 5, Additional File 3). These data  
342 demonstrate high correlation between GPSs from lcWGS data and genotyping array in a  
343 randomly selected sample. Interestingly, correlation at 0.1X was still high enough that GPSs at  
344 this coverage may have research utility, suggesting that significant amounts of data regarding  
345 common genetic variation could be recovered from off-target reads in exome and multi-gene

346 panel sequencing studies to allow for GPS calculation. Taken together, these data demonstrate  
347 that lcWGS provides equivalent accuracy for calculation of GPSs, with sequencing coverage as  
348 low as 0.5X.

349

### 350 **Assessment of imputation performance and technical concordance across diverse** 351 **populations**

352 To further assess the performance of our imputation pipeline across diverse populations, we  
353 performed lcWGS on 120 additional samples from six 1KGP populations (CHB, GIH, YRI, ASW,  
354 MXL, and PUR; see Supplementary Table 3, Additional File 1) that represent the range of  
355 ancestry observed in admixed populations (diverse ancestry data set). We compared genotypes  
356 imputed using our lcWGS pipeline to known 1KGP WGS data and found that imputation  
357 accuracy was above 0.90  $r^2$  for all samples (range 0.94 - 0.97) (Figure 4A). In addition, we  
358 found that GPS calculated from lcWGS data and GPS calculated from the Phase 3 1KGP WGS  
359 data release have a high correlation, with an  $r^2$  value of 0.98, 0.91, and 0.98 for CAD, BC, and  
360 AF, respectively (Figure 4B-D). These results suggest that lcWGS can enable accurate  
361 imputation and calculation of GPSs in diverse populations.

362

### 363 **Association of lcWGS-calculated GPSs with disease phenotypes in a clinical cohort**

364 Previous studies have demonstrated the association of GPSs with prevalent disease using  
365 genotyping arrays [3,8,20–22] and hcWGS [16]. To observe the performance of lcWGS-  
366 calculated GPSs in a large population, we performed low coverage sequencing on 11,502  
367 European individuals (clinical cohort) (See Supplementary Table 2, Additional File 1) and  
368 calculated  $GPS_{CAD}$ ,  $GPS_{BC}$ , and  $GPS_{AF}$  for each individual. Raw GPSs were normalized by  
369 taking the standardized residual of the predicted score after correction for the first 10 PCAs (see  
370 Supplementary Figure 6, Additional File 3) [16,23]. First, we note that there are no major outliers  
371 (defined as a z-score greater than 5) in  $GPS_{CAD}$ ,  $GPS_{BC}$ , and  $GPS_{AF}$  and that the normalized

372 scores formed an approximately normal distribution for each (see Supplementary Figure 7,  
373 Additional File 3). Each of the GPSs were strongly associated with self-reported history of  
374 disease, with effect estimates comparable to prior reports using genotyping arrays to calculate  
375 GPS -- GPS<sub>CAD</sub> (OR per standard deviation = 1.59 (1.32 - 1.92), n = 11,010), GPS<sub>BC</sub> (OR per  
376 standard deviation = 1.56 (1.45 - 1.68); n = 8722), and GPS<sub>AF</sub> (OR per standard deviation =  
377 1.28 (1.12 - 1.46); n = 10,303) (Figure 5).

378  
379 Previous studies have noted significantly increased disease prevalence among individuals in the  
380 extreme tails of the GPS distribution when compared to the remainder of the population [3,8].  
381 We replicated this observation by assessing the prevalence of disease in the highest 5% of the  
382 GPS distribution for each of the three diseases, noting odds ratios of 4.5 (2.62 - 7.74), 2.62  
383 (2.04 - 3.36), and 1.96 (1.24 - 3.11) for GPS<sub>CAD</sub>, GPS<sub>BC</sub>, and GPS<sub>AF</sub>, respectively.

384  
385 Area under the curve (AUC) is an additional metric used to assess the ability of a given risk  
386 factor to discriminate between affected cases and disease-free controls. When only the GPS  
387 was included in the prediction model, GPS<sub>CAD</sub> had an AUC of 0.60, GPS<sub>BC</sub> had an AUC of 0.63,  
388 and GPS<sub>AF</sub> had an AUC of 0.57. The additional inclusion of age and sex increased the AUCs to  
389 0.86 for GPS<sub>CAD</sub>, 0.78 for GPS<sub>BC</sub>, and 0.78 for GPS<sub>AF</sub>. For each of these three common,  
390 complex diseases, the magnitude of associations with clinical disease and AUC metrics were  
391 consistent with previous publications [3,8]. Taken together, these results suggest that lcWGS-  
392 calculated GPSs can accurately stratify risk with comparable accuracy to previously published  
393 GPS-disease associations calculated on the basis of genotyping array data.

## 394 395 **DISCUSSION**

396 For the past two decades, genotyping array-based GWAS and imputation have been the driving  
397 force in our discovery of genetic loci predictive of disease and derivation and calculation of



398 GPSs. In this study, we developed and validated an imputation pipeline to calculate GPSs from  
399 variably downsampled hcWGS and lcWGS data sets. While the efficiency of lcWGS has been  
400 reported for other applications of statistical genetics [4–6], we demonstrate that lcWGS achieves  
401 similar technical concordance as the Axiom UK Biobank Array by Affymetrix for determining  
402 GPSs. Furthermore, the imputation  $r^2$  from lcWGS was greater than 90%, which is similar to the  
403 imputation accuracy reported from other commercially-available genotyping arrays [24]. Taken  
404 together, these data suggest that lcWGS has comparable accuracy to genotyping arrays for  
405 assessment of common variants and subsequent calculation of GPSs.

406  
407 Our finding that lcWGS can be used for accurate genotyping and imputation of common genetic  
408 variants has implications for the future of genomic research and medicine. Currently, disease  
409 GWAS are performed using a variety of genotyping arrays that are designed to target specific  
410 sets of genes or features, reducing imputation quality in regions that are not targeted [25].  
411 lcWGS enables less biased imputation than genotyping arrays by not pre-specifying the genetic  
412 content that is included for assessment, as is necessary for genotyping arrays. Because initial  
413 GWAS focused on populations with high homogeneity to reduce noise and increase fit of risk  
414 stratification, many genotyping arrays were designed to capture common genetic variants based  
415 on the linkage disequilibrium structure in European populations [26]. However, this  
416 ascertainment bias reduces the imputation performance from genotyping array data in diverse  
417 populations [27–29]. Imputation from lcWGS data reduces this bias by including all SNPs  
418 observed in 1KGP populations as potential predictors. The effects of SNP selection bias are  
419 also not equivalent across genotyping arrays, and therefore variants included in a GPS trained  
420 and validated on one genotyping array may not be as predictive on another genotyping array  
421 [30]. lcWGS systematically surveys variants independent of SNP selection bias and thus  
422 provides one approach to overcome this issue. Our findings here demonstrate that GPSs  
423 trained and validated on different genotyping arrays are transferable to lcWGS-calculated GPS.

424 Furthermore, as new genetic associations are discovered, lcWGS can be re-analyzed with ever  
425 more inclusive sets of known SNPs, further reducing SNP selection bias and advancing the  
426 study and understanding of the genetic contributions to disease. In contrast, genotyping arrays  
427 are static and cannot be easily updated or changed without designing a *de novo* platform.

428

429 lcWGS also has the potential to easily integrate into current clinical sequencing pipelines. In  
430 contrast to genotyping arrays, which require investment in separate laboratory technology,  
431 lcWGS can be performed on the same platform as current hcWGS or targeted multi-gene panel  
432 clinical testing. The ease of combining these two pathways could help to drive GPS adoption  
433 into clinical practice and can likely be achieved at a cost comparable to genotyping arrays [4].  
434 As the cost of next generation sequencing continues to decrease, the cost of lcWGS will also  
435 continue to decrease.

436

437 This study should be interpreted in the context of potential limitations. First, the imputation  
438 accuracy observed in our analysis may have been limited by the reference panel size. Future  
439 efforts using an even larger reference panel may lead to further improved imputation accuracy,  
440 particularly for variants with allele frequency less than 1% [24]. Second, while lcWGS may  
441 ultimately enable derivation of GPSs with improved predictive accuracy or ethnic transferability,  
442 this was not explicitly explored here. Rather, we demonstrate the feasibility and accuracy of  
443 using lcWGS of calculating GPSs published in previous studies. Third, disease phenotypes in  
444 our clinical cohort were based on individual self-report rather than review of health records.  
445 However, several studies have shown that self-reported personal history data have high  
446 concordance with data reported by a healthcare provider or electronic health records [31–34],  
447 and any inaccuracies would be expected to bias GPS-disease associations to the null.

448

449 **CONCLUSIONS**

450 In conclusion, this work establishes lcWGS as an alternative approach to genotyping arrays for  
451 common genetic variant assessment and GPS calculation -- providing comparable accuracy at  
452 similar cost while also overcoming the ascertainment bias inherent to variant selection in  
453 genotyping array design.

454

## 455 **LIST OF ABBREVIATIONS**

456 GPS, genome-wide polygenic score

457 lcWGS, low coverage whole genome sequencing

458 CAD, coronary artery disease

459 BC, breast cancer

460 AF, atrial fibrillation

461 1KGP, 1000 Genomes Project

462 GIAB, Genome in a Bottle

463 Indel, insertion-deletion

464 BWA, Burrows-Wheeler Aligner

465 IBS, Identity-by-State

466 PC, principal components

467 PCA, PC analysis

468 MAF, minor allele frequency

469 AUC, area under the curve

470

## 471 **DECLARATIONS**

### 472 **Ethics approval and consent to participate**

473 All individuals in the technical concordance cohort and clinical cohort gave electronic informed

474 consent to have their de-identified information and sample used in anonymized studies

475 (Western Institutional Review Board, #20150716).

476

477 **Consent for publication**

478 All individuals in the technical concordance cohort and clinical cohort gave electronic informed  
479 consent that Color may author publications using non-aggregated, de-identified information,  
480 either on its own or in collaboration with academic or commercial third parties.

481

482 **Availability of data and material**

483 The technical concordance and clinical cohort data are not publicly available given the potential  
484 to compromise research participant privacy or consent.

485

486 1KGP, <http://www.internationalgenome.org/>

487 GIAB, <ftp://ftp-trace.ncbi.nlm.nih.gov/giab/ftp/release/AshkenazimTrio/>

488 Samtools/Bcftools, <http://www.htslib.org/>

489 BEAGLE, <https://faculty.washington.edu/browning/beagle/beagle.html>

490 FastNGSAdmix, <http://www.popgen.dk/software/index.php/FastNGSAdmix>

491

492 **Competing interests**

493 JRH, CLN, and AYZ are currently employed by and have equity interest in Color Genomics.

494 JRH has previously consulted for Twist Bioscience and Etalon Diagnostics. GM was previously

495 employed at Color Genomics and Operator. JRH and GM report a patent application related to

496 low coverage whole genome sequencing. SK is an employee of Verve Therapeutics and holds

497 equity in Verve Therapeutics, Maze Therapeutics, Catabasis, and San Therapeutics. He is a

498 member of the scientific advisory boards for Regeneron Genetics Center and Corvidia

499 Therapeutics; he has served as a consultant for Acceleron, Eli Lilly, Novartis, Merck, Novo

500 Nordisk, Novo Ventures, Ionis, Alnylam, Aegerion, Haug Partners, Noble Insights, Leerink

501 Partners, Bayer Healthcare, Illumina, Color Genomics, MedGenome, Quest, and Medscape; he

502 reports patents related to a method of identifying and treating a person having a predisposition  
503 to or afflicted with cardiometabolic disease (20180010185) and a genetic risk predictor  
504 (20190017119). AVK has served as a consultant for Color Genomics and reports a patent  
505 related to a genetic risk predictor (20190017119).

506

#### 507 **Funding**

508 This work was supported by Color Genomics.

509

#### 510 **Authors' contributions**

511 JRH, GM, AYZ, and AVK designed the overall study. JRH, CLN, GM, AYZ, SK, and AVK  
512 contributed to data acquisition and analysis. JRH, CLN, GM, AYZ, SK, and AVK drafted or  
513 critically revised the manuscript for important intellectual content. AYZ and AVK are the  
514 guarantors of this work and, as such, have full access to all of the data in the study and take  
515 responsibility for the integrity of the data and the accuracy of the data analysis.

516

#### 517 **Acknowledgements**

518 We would like to thank Will Stedden, Carmen Lai, and Anjali D. Zimmer for helpful discussions  
519 and Justin Lock, Alok Sabnis, and Valerie Ngo for laboratory support and sample processing.

520 **REFERENCES**

- 521 1. Lozano R, Naghavi M, Foreman K, Lim S, Shibuya K, Aboyans V, et al. Global and regional  
522 mortality from 235 causes of death for 20 age groups in 1990 and 2010: a systematic analysis  
523 for the Global Burden of Disease Study 2010. *Lancet*. 2012;380:2095–128.
- 524 2. Boyle EA, Li YI, Pritchard JK. An Expanded View of Complex Traits: From Polygenic to  
525 Omnigenic. *Cell*. 2017;169:1177–86.
- 526 3. Khera AV, Chaffin M, Aragam KG, Haas ME, Roselli C, Choi SH, et al. Genome-wide  
527 polygenic scores for common diseases identify individuals with risk equivalent to monogenic  
528 mutations. *Nat Genet* [Internet]. 2018; Available from: [http://dx.doi.org/10.1038/s41588-018-](http://dx.doi.org/10.1038/s41588-018-0183-z)  
529 0183-z
- 530 4. Pasaniuc B, Rohland N, McLaren PJ, Garimella K, Zaitlen N, Li H, et al. Extremely low-  
531 coverage sequencing and imputation increases power for genome-wide association studies. *Nat*  
532 *Genet*. 2012;44:631–5.
- 533 5. Gilly A, Southam L, Suveges D, Kuchenbaecker K, Moore R, Melloni GEM, et al. Very low  
534 depth whole genome sequencing in complex trait association studies. *Bioinformatics* [Internet].  
535 2018; Available from: <http://dx.doi.org/10.1093/bioinformatics/bty1032>
- 536 6. Liu S, Huang S, Chen F, Zhao L, Yuan Y, Francis SS, et al. Genomic Analyses from Non-  
537 invasive Prenatal Testing Reveal Genetic Associations, Patterns of Viral Infections, and  
538 Chinese Population History. *Cell*. 2018;175:347–59.e14.
- 539 7. Navon O, Sul JH, Han B, Conde L, Bracci PM, Riby J, et al. Rare variant association testing  
540 under low-coverage sequencing. *Genetics*. 2013;194:769–79.
- 541 8. Mavaddat N, Michailidou K, Dennis J, Lush M, Fachal L, Lee A, et al. Polygenic Risk Scores

- 542 for Prediction of Breast Cancer and Breast Cancer Subtypes. *Am J Hum Genet.* 2019;104:21–  
543 34.
- 544 9. Jørsboe E, Hanghøj K, Albrechtsen A. fastNGSadmix: admixture proportions and principal  
545 component analysis of a single NGS sample. *Bioinformatics.* 2017;33:3148–50.
- 546 10. Neben CL, Zimmer AD, Stedden W, van den Akker J, O'Connor R, Chan RC, et al. Multi-  
547 Gene Panel Testing of 23,179 Individuals for Hereditary Cancer Risk Identifies Pathogenic  
548 Variant Carriers Missed by Current Genetic Testing Guidelines. *J Mol Diagn [Internet]. Elsevier;*  
549 2019 [cited 2019 Jun 11];0. Available from: <https://jmd.amjpathol.org/article/S1525->  
550 1578(18)30334-9/fulltext
- 551 11. Li H, Handsaker B, Wysoker A, Fennell T, Ruan J, Homer N, et al. The Sequence  
552 Alignment/Map format and SAMtools. *Bioinformatics.* 2009;25:2078–9.
- 553 12. Li H. Aligning sequence reads, clone sequences and assembly contigs with BWA-MEM  
554 [Internet]. *arXiv [q-bio.GN].* 2013. Available from: <http://arxiv.org/abs/1303.3997>
- 555 13. Li H. A statistical framework for SNP calling, mutation discovery, association mapping and  
556 population genetical parameter estimation from sequencing data. *Bioinformatics.* 2011;27:2987–  
557 93.
- 558 14. Browning BL, Browning SR. Genotype Imputation with Millions of Reference Samples. *Am J*  
559 *Hum Genet.* 2016;98:116–26.
- 560 15. Browning BL, Zhou Y, Browning SR. A One-Penny Imputed Genome from Next-Generation  
561 Reference Panels. *Am J Hum Genet.* 2018;103:338–48.
- 562 16. Khera AV, Chaffin M, Zekavat SM, Collins RL, Roselli C, Natarajan P, et al. Whole Genome  
563 Sequencing to Characterize Monogenic and Polygenic Contributions in Patients Hospitalized

- 564 with Early-Onset Myocardial Infarction. *Circulation* [Internet]. American Heart Association  
565 Bethesda, MD; 2018 [cited 2018 Nov 27]; Available from:  
566 <https://www.ahajournals.org/doi/abs/10.1161/CIRCULATIONAHA.118.035658>
- 567 17. Wang C, Zhan X, Liang L, Abecasis GR, Lin X. Improved ancestry estimation for both  
568 genotyping and sequencing data using projection procrustes analysis and genotype imputation.  
569 *Am J Hum Genet.* 2015;96:926–37.
- 570 18. Lazaridis I, Nadel D, Rollefson G, Merrett DC, Rohland N, Mallick S, et al. Genomic insights  
571 into the origin of farming in the ancient Near East. *Nature.* 2016;536:419–24.
- 572 19. 1000 Genomes Project Consortium, Auton A, Brooks LD, Durbin RM, Garrison EP, Kang  
573 HM, et al. A global reference for human genetic variation. *Nature.* 2015;526:68–74.
- 574 20. Inouye M, Abraham G, Nelson CP, Wood AM, Sweeting MJ, Dudbridge F, et al. Genomic  
575 Risk Prediction of Coronary Artery Disease in 480,000 Adults: Implications for Primary  
576 Prevention. *J Am Coll Cardiol.* 2018;72:1883–93.
- 577 21. Richardson TG, Harrison S, Hemani G, Smith GD. An atlas of polygenic risk score  
578 associations to highlight putative causal relationships across the human phenome [Internet].  
579 bioRxiv. 2018 [cited 2018 Nov 27]. p. 467910. Available from:  
580 <https://www.biorxiv.org/content/early/2018/11/11/467910>
- 581 22. Mavaddat N, Pharoah PDP, Michailidou K, Tyrer J, Brook MN, Bolla MK, et al. Prediction of  
582 breast cancer risk based on profiling with common genetic variants. *J Natl Cancer Inst* [Internet].  
583 2015;107. Available from: <http://dx.doi.org/10.1093/jnci/djv036>
- 584 23. Price AL, Patterson NJ, Plenge RM, Weinblatt ME, Shadick NA, Reich D. Principal  
585 components analysis corrects for stratification in genome-wide association studies. *Nat Genet.*  
586 2006;38:904–9.



- 587 24. McCarthy S, Das S, Kretzschmar W, Delaneau O, Wood AR, Teumer A, et al. A reference  
588 panel of 64,976 haplotypes for genotype imputation. *Nat Genet.* 2016;48:1279–83.
- 589 25. Voight BF, Kang HM, Ding J, Palmer CD, Sidore C, Chines PS, et al. The metabochip, a  
590 custom genotyping array for genetic studies of metabolic, cardiovascular, and anthropometric  
591 traits. *PLoS Genet.* 2012;8:e1002793.
- 592 26. Lachance J, Tishkoff SA. SNP ascertainment bias in population genetic analyses: why it is  
593 important, and how to correct it. *Bioessays.* 2013;35:780–6.
- 594 27. Wojcik GL, Fuchsberger C, Taliun D, Welch R, Martin AR, Shringarpure S, et al. Imputation-  
595 Aware Tag SNP Selection To Improve Power for Large-Scale, Multi-ethnic Association Studies.  
596 *G3.* 2018;8:3255–67.
- 597 28. Nelson SC, Doheny KF, Pugh EW, Romm JM, Ling H, Laurie CA, et al. Imputation-Based  
598 Genomic Coverage Assessments of Current Human Genotyping Arrays [Internet]. *G3:*  
599 *Genes|Genomes|Genetics.* 2013. p. 1795–807. Available from:  
600 <http://dx.doi.org/10.1534/g3.113.007161>
- 601 29. Carlson CS, Matise TC, North KE, Haiman CA, Fesinmeyer MD, Buyske S, et al.  
602 Generalization and dilution of association results from European GWAS in populations of non-  
603 European ancestry: the PAGE study. *PLoS Biol.* 2013;11:e1001661.
- 604 30. Johnson EO, Hancock DB, Levy JL, Gaddis NC, Saccone NL, Bierut LJ, et al. Imputation  
605 across genotyping arrays for genome-wide association studies: assessment of bias and a  
606 correction strategy. *Hum Genet.* 2013;132:509–22.
- 607 31. Gentry-Maharaj A, Fourkala E-O, Burnell M, Ryan A, Apostolidou S, Habib M, et al.  
608 Concordance of National Cancer Registration with self-reported breast, bowel and lung cancer  
609 in England and Wales: a prospective cohort study within the UK Collaborative Trial of Ovarian

610 Cancer Screening. Br J Cancer. 2013;109:2875–9.

611 32. D’Aloisio AA, Nichols HB, Hodgson ME, Deming-Halverson SL, Sandler DP. Validity of self-  
612 reported breast cancer characteristics in a nationwide cohort of women with a family history of  
613 breast cancer. BMC Cancer. 2017;17:692.

614 33. Kehoe R, Wu SY, Leske MC, Chylack LT Jr. Comparing self-reported and physician-  
615 reported medical history. Am J Epidemiol. 1994;139:813–8.

616 34. Malmö V, Langhammer A, Børnaa KH, Loennechen JP, Ellekjaer H. Validation of self-  
617 reported and hospital-diagnosed atrial fibrillation: the HUNT study. Clin Epidemiol. 2016;8:185–  
618 93.

619

620 **ADDITIONAL FILES**

621 Additional File 1

622 Homburger et al Additional File 1, PDF

623 Supplementary tables and legends

624

625 Additional File 2

626 Homburger et al Additional File 2, PDF

627 Supplementary Methods

628

629 Additional File 3

630 Homburger et al Additional File 3, PDF

631 Supplementary figures and legends

632

633 **FIGURE TITLES AND LEGENDS**

634 Figure 1. Study design and imputation pipelines. The study design has four groups: (A) pipeline  
635 validation data set and (B) technical concordance cohort, diverse ancestry data set, and clinical  
636 cohort. The imputation pipeline for each group is depicted. hcWGS, high coverage whole  
637 genome sequencing. lcWGS, low coverage whole genome sequencing. HWE, Hardy–Weinberg  
638 equilibrium. GPS, genome-wide polygenic score. CAD, coronary artery disease. BC, breast  
639 cancer. AF, atrial fibrillation.

640

641 Figure 2. Assessment of imputation performance in the pipeline validation data set.

642 Downsampling from 30X to 0.1X showed that lcWGS accuracy was above 0.90  $r^2$  for all  
643 samples at 0.5X ( $n = 4$  independent random seeds for each sample and coverage value; error  
644 bars are 95% confidence intervals). The thick brown dashed line is a smoothed trendline of the  
645 average imputation quality while the thin grey dashed line demonstrates previously reported  
646 imputation quality from a genotyping array ( $r^2 = 0.90$ ) [4]. AJ, Ashkenazi Jewish. CDX, Chinese  
647 Dai in Xishuangbanna, China. CEU, Utah Residents with Northern and Western European  
648 Ancestry. CHB, Han Chinese in Beijing, China. CLM, Colombians from Medellin, Colombia.  
649 GIH, Gujarati Indian from Houston, Texas. TSI, Toscani in Italia. YRI, Yoruba in Ibadan, Nigeria.

650

651 Figure 3. Correlation of GPSs between genotyping array and lcWGS in the technical  
652 concordance cohort. (A)  $\text{GPS}_{\text{CAD}}$  calculated using lcWGS was highly correlated ( $r^2 = 0.98$ ) with  
653 those calculated using genotyping array ( $n = 182$ ). (B)  $\text{GPS}_{\text{BC}}$  calculated using lcWGS was  
654 highly correlated ( $r^2 = 0.93$ ) with those calculated using genotyping array ( $n = 182$ ). (C)  $\text{GPS}_{\text{AF}}$   
655 was highly correlated ( $r^2 = 0.97$ ) with those calculated using genotyping arrays ( $n = 182$ ). x-axis  
656 is the raw GPS calculated from the genotyping array, and y-axis is the raw GPS calculated from  
657 the lcWGS data; raw GPS values are unitless. lcWGS, low coverage whole genome

658 sequencing. GPS, genome-wide polygenic score. CAD, coronary artery disease. BC, breast  
659 cancer. AF, atrial fibrillation.

660

661 Figure 4. Assessment of imputation performance and technical concordance across diverse  
662 populations. (A)  $GPS_{CAD}$  calculated using lcWGS data was highly correlated with those  
663 calculated using known 1KGP data ( $n = 116$ ), with all samples having a correlation coefficient  
664 above 0.90. The thin grey dashed line demonstrates previously reported imputation quality from  
665 a genotyping array ( $r^2 = 0.90$ ) [4]. (B)  $GPS_{CAD}$  calculated using lcWGS data was highly  
666 correlated ( $r^2 = 0.98$ ) with those calculated using known 1KGP data ( $n = 116$ ). (C)  $GPS_{BC}$   
667 calculated using lcWGS data was highly correlated ( $r^2 = 0.91$ ) with those calculated using  
668 known 1KGP data ( $n = 116$ ). (D)  $GPS_{AF}$  was highly correlated ( $r^2 = 0.98$ ) with those calculated  
669 using known 1KGP data ( $n = 116$ ). 1KGP, 1000 Genomes Project. lcWGS, low coverage whole  
670 genome sequencing. GPS, genome-wide polygenic score. CAD, coronary artery disease. BC,  
671 breast cancer. AF, atrial fibrillation.

672

673 Figure 5. Association of lcWGS-calculated GPSs with disease phenotypes in the clinical cohort.  
674 lcWGS-calculated  $GPS_{CAD}$  was associated with personal history of CAD (OR = 1.589 (1.32 -  
675 1.92),  $n = 11,010$ ,  $p = 1.32 \times 10^{-6}$ ).  $GPS_{CAD}$  was adjusted for age and sex. lcWGS-calculated  
676  $GPS_{BC}$  was associated with personal history of BC (OR = 1.56 (1.45 - 1.68);  $n = 8,722$ ,  $p = 1.0 \times$   
677  $10^{-16}$ ).  $GPS_{BC}$  was calculated only for females and adjusted for age at menarche. lcWGS-  
678 calculated  $GPS_{AF}$  was associated with personal history of AF (OR = 1.277 (1.12 - 1.46);  $n =$   
679  $10,303$ ,  $p = 0.000292$ ).  $GPS_{AF}$  was adjusted for age and sex. lcWGS, low coverage whole  
680 genome sequencing. GPS, genome-wide polygenic score. CAD, coronary artery disease. BC,  
681 breast cancer. AF, atrial fibrillation.

# Figure 1

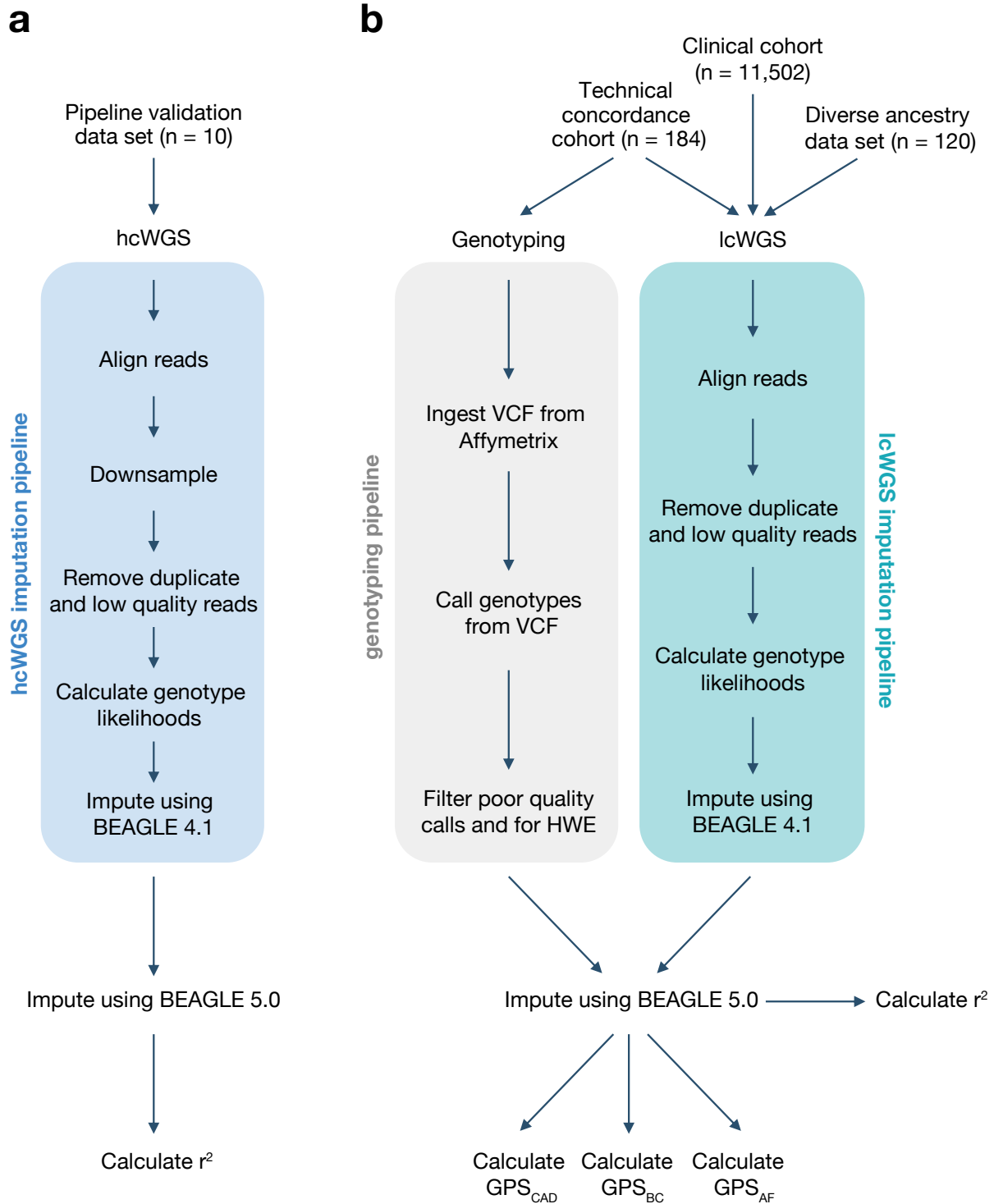


# Figure 2

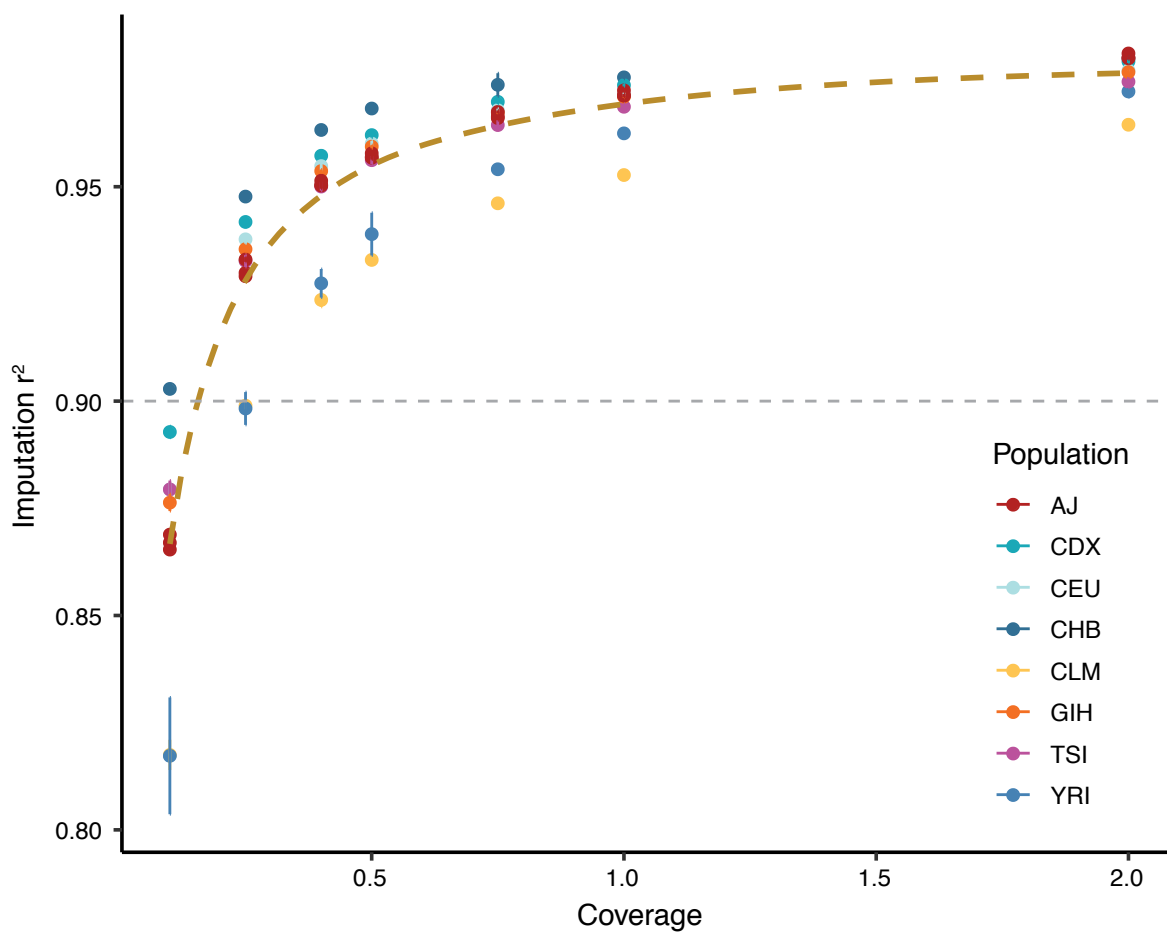


Figure 3

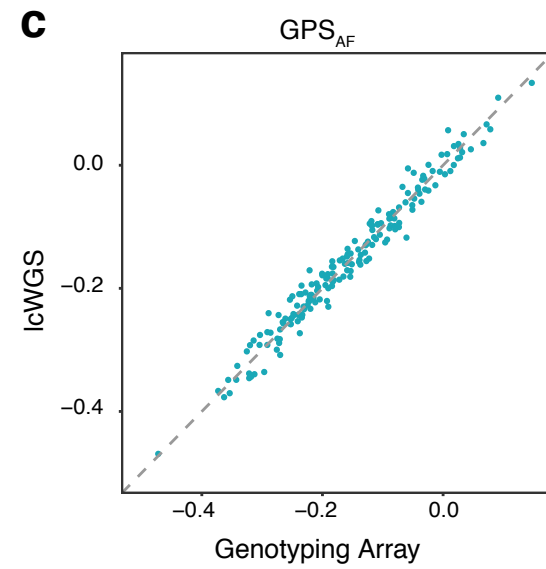
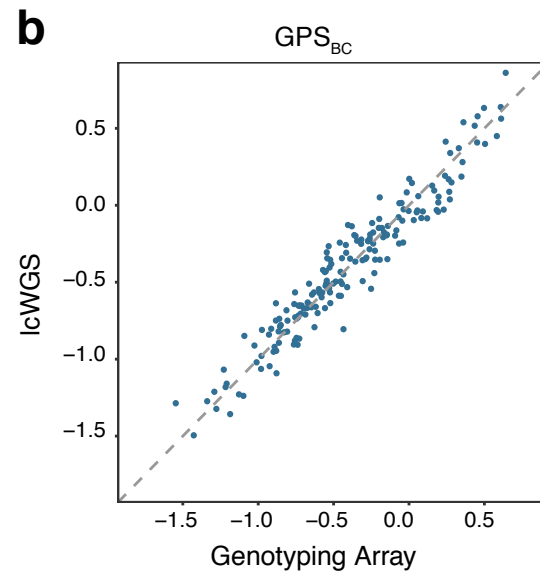
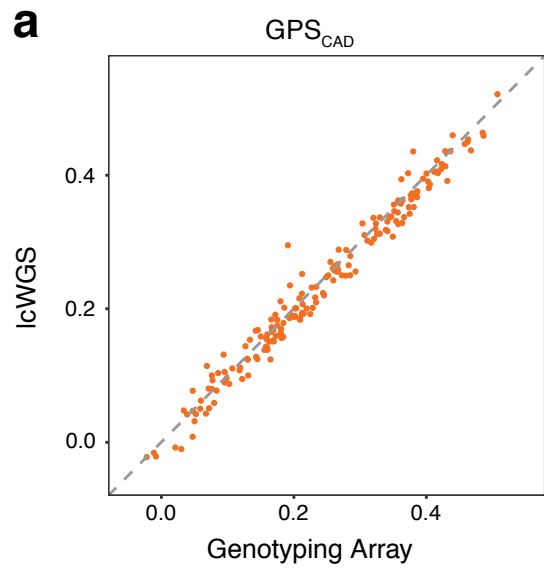
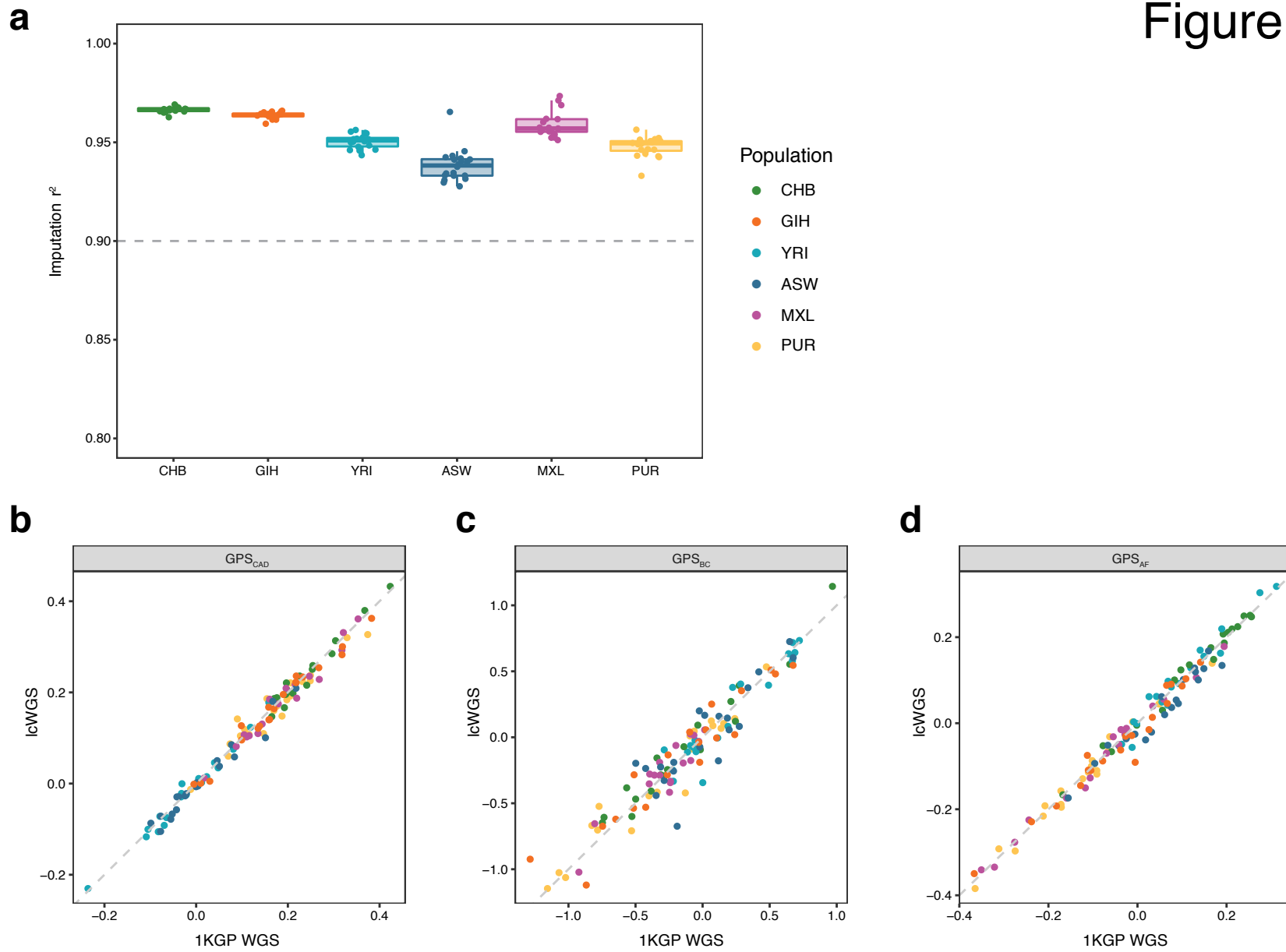


Figure 4





## Figure 5

